1* Hussein Mohammed Aesa

² Sadjad A. Hemzeh

³ Aymen J Alsaad

Experimental Investigation of Flexural Behavior of Hybrid Self-Compacting Pozzo-Lime Reinforced Concrete Beams



Abstract: - The main goal of this research is to investigate the effect of using hybrid self-compacting Pozzo-lime concrete on the bending behaviour of reinforced concrete beams. To achieve this objective, a set of eight laboratory samples comprised of reinforced concrete beams measuring 1400 mm in length and 150 x 250 mm in dimensions were subjected to two-point bending testing. These beams were constructed using hybrid self-compacting Pozzo-lime concrete at varying depths. The samples' ultimate strength, ductility, cracking pattern, and mode of failure, as well as the load-displacement diagram, are subsequently assessed. The laboratory sample of the P75C25 beam exhibited the greatest final strength, hardness, and ductility, according to the findings of this study.

Keywords: Hybrid self-compacting Pozzo-lime concrete, ultimate strength, ductility, failure mode, cracking.

I. INTRODUCTION

Time, cost, and quality are three vital determinants in the implementation stage that significantly influence the construction sector. Civil engineers are invariably intrigued by any advancement or progression that enhances these three factors (1-4). When these developments become feasible in the construction industry, adequate research should be conducted to determine their benefits and drawbacks, and the required steps should be taken to implement them (5-8). Due to its special characteristics, self-compacting concrete is one of these developments that can have a significant impact on the construction industry (9-11). Engineers from various nations have aspired for many years to develop self-levelling concrete (self-compacting) that does not degrade in fluidity, strength, or separation. When the concrete mix was dry at the turn of the 20th century, the only way to compact it was through the use of heavy impacts (12-15). It was feasible in expansive and accessible segments (16-18). In the 1920s, it was determined that an increase in the water-cement ratio could result in a reduction in the strength of the concrete (19, 20). This trend toward wetter mixes gained traction as the use of reinforced concrete became more widespread, and the practical issues associated with dry mixes became more apparent (21, 22). The detrimental impact of increasing the water-cement ratio on the permeability and durability of concrete was further exposed in subsequent years as concerns regarding the durability of concrete were further examined (23).

All this caused special attention to be paid to concrete performance and rheology properties as well as compaction methods, with the aim of improving its strength and durability properties (24, 25). This research finally led to the introduction of self-compacting concrete in Japan. Concrete with high flowability that can fill all the corners of the mould and include the reinforcements only under the influence of gravity and without the need to perform any other process, without causing separation or water leakage. Investigation of rheology and efficiency shows a high impact on determining the properties of self-compacting concrete (26).

So far, a lot of research has been done in the field of self-compacting concrete, including Saha et al. (27), Afshoon et al. (28), Kassimi et al. (29), Nawaz (25), Ashteyat et al. (30) studies, none of which investigated the effect of Hybrid Self-Compacting Pozzo-Lime concrete. Consequently, research into Hybrid Self-Compacting Pozzo-Lime concrete is still in its early stages. Determining the impact of Hybrid Self-Compacting Pozzo-Lime concrete on the ultimate strength, ductility, and hardness of reinforced concrete beams is thus the goal of this investigation, which attempts to address this scientific gap. Also, this research investigates the pattern of cracking and breaking mode of the reinforced concrete beam with Hybrid Self-Compacting Pozzo-Lime concrete. To achieve the goal of this research and to find appropriate answers to the research questions, eight samples of reinforced concrete beams with geometric specifications and reinforcement details are tested under four-point bending, and the results are examined.

II. EXPERIMENTAL PROGRAM

Materials

¹ MSc student in Structure Engineering, Department of Civil Engineering, Faculty of Engineering, Kerbala University, Kerbala, Iraq.

² Professor, Department of Civil Engineering, Faculty of Engineering, Kerbala University, Kerbala, Iraq.

³ Assistant Professor, Department of Civil Engineering, Faculty of Engineering, Kerbala University, Kerbala, Iraq.

^{*}Corresponding author: Hussein Mohammed Aesa

The water utilised in this study satisfies all international standards for cleanliness. The cement used in all the mixing plants is medium anti-sulphate Portland cement (type two) from the Karbala cement factory. According to the tests, all the specifications of the cement used are entirely in accordance with the required standards in Iraq.

Also, in this research, concrete from hydrated lime manufactured by Karbala Lime Company, whose specifications are according to the Iraqi standard [IQS No. 807/2004], is used. The micro silica used in this research is Mega-Add MS(D) manufactured by CONMIX Construction Chemical Company, and its specifications are in accordance with ASTM-C1240 standards. The aggregates used in the tests were from the same depot all the time, and all the tests needed to validate the aggregates, as one of the most important components of concrete, were performed on them. The sand used is washed and crushed sand from the mines of Karbala city. Granulation specifications for the sand used in this research are shown in Table 1.

Table 1. Characteristics of fine and coarse aggregate granulation.

	Sieve Size (mm)	Cumulative passing (%)	IQS No.45- 1984
Coarse	37.5	100	-
Aggregate	25	100	-
	20	100	100
	14	100	100-90
	10	79	85-50
	5	8.8	10-0
	2.33	2.3	-
Fine Aggregate	10	100	100
	4.75	97	100-90
	2.36	91	85-100
	1.18	85	90-75
	0.6	76	79-60
	0.3	40	40-12
	0.18	10	0-10

The super-lubricant used in this research is a light brown liquid, and its physical and chemical characteristics are in accordance with ASTM-C494. Figure 1 shows the materials used in this research.



Figure 1. Materials used in this research.

High – Range Water Reducing Admixture

Hydrated Lime

Mixing plan and mechanical characteristics of concretes

In this research, two types of concrete, including Hybrid Self-Compacting Pozzo-Lime concrete and ordinary Self-Compacting concrete, have been investigated, and their mixing plan for one cubic meter of concrete is shown in Table 2.

Table 2. Mix design for 1m³ concrete.

Mix	Binder			Sand Kg/m ³	Gravel Kg/m³	W/B ratio	SP
	С	HL	SF	Kg/III*	Kg/III*		
C (Ref.)	450	0	0	800	850	38%	2.5
P60	220	165	165	700	850	42%	2.5

The compressive strength, tensile strength, and bending strength of laboratory samples that had been hardened were assessed in this study. Initial determination of the compressive strength is conducted in accordance with BS EN-12390 using 100 mm cubes. The subsequent procedure involved conducting the Brazilian tensile strength test on cylindrical specimens measuring 200x200 mm in accordance with the ASTM-C496 standard. In the final stage, 500x100x100 mm prismatic samples are utilised, and the bending strength is determined using the four-point bending method in accordance with the ASTM-C293 standard. The mechanical characteristics of concrete samples are detailed in Table 3.

Table 3. Mechanical characteristics of concrete samples.

Mix design	Compressive strength (Mpa)		Splitting ten	sile strength (Mpa)	Flexural strength (Mpa)
Age	7 day	28 day	7 day	28 day	28 day
Reff	26.7	35.6	3.1	3.7	4.0
P60	22.3	34.4	2.4	3.0	3.8

Details of reinforced concrete beam laboratory samples

In this research, eight laboratory samples whose names are shown in Table 4 were made according to the details shown in Figure 2. Also, the steps of manufacturing reinforced concrete beam laboratory samples are shown in Figure 3.

Table 4. Nomenclature of reinforced concrete beam laboratory samples.

Specimen	Specification
C100(Reff)	beam constructed using a full self-compacting concert
C75P25	beam constructed using (75%) self-compacting concrete (from height, from bottom) and
	(25%) self-compacting pozzolim concert
C50P50	beam constructed using (50%) self-compacting concrete (from height, from bottom) and
	(50%) self-compacting pozzolim concert
C25P75	beam constructed using (25%) self-compacting concrete (from height, from bottom) and
	(75%) self-compacting pozzolim concert
P100	constructed using full self-compacting pozzolim concert
P75C25	beam constructed using (75%) self-compacting pozzolim concrete (from height, from
	bottom) and (25%) self-compacting concert
P50C50	beam constructed using (50%) self-compacting pozzolim concrete (from height, from
	bottom) and (50%) self-compacting concert
P25C75	beam constructed using (25%) self-compacting pozzolim concrete (from height, from
	bottom) and (75%) self-compacting concert

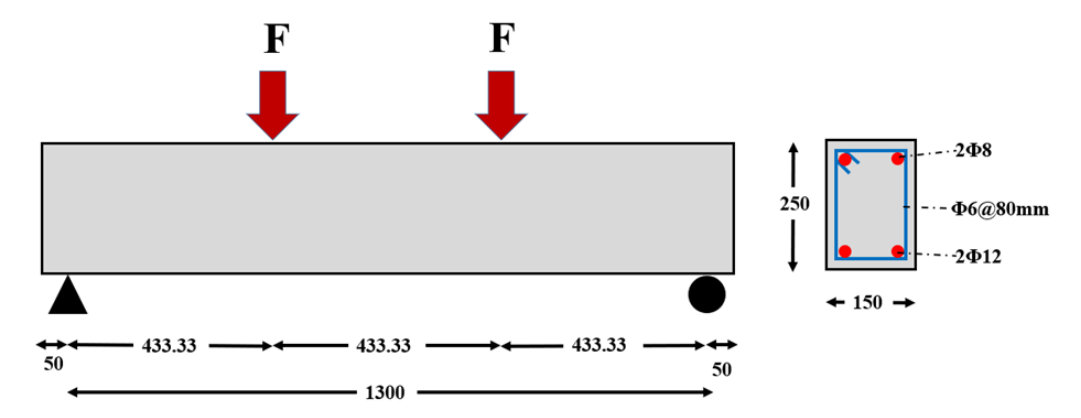


Figure 2. Geometric specifications and reinforcement details of reinforced concrete beam laboratory samples.



Figure 3. Steps of making laboratory samples of reinforced concrete beam.

Laboratory setup

The reinforced concrete laboratory samples were tested in four-point bending using a hydraulic jack. The four-point bending test is one of the best and most common beam tests. In this test, the area between two-point loads has constant anchorage and zero shear. Therefore, in this area, it is possible to investigate the behaviour of the beam under pure bending. In the area between each of the point loads and the closest support to that load, the effect of bending and cutting can also be checked. The loading was carried out as a static and uniform load. The displacement of the middle of the beam was transferred by the linear displacement transducer (LVDT), the force was transferred to the data recording device by the dynamometer, and the experimental deflection of the laboratory samples was taken in the middle of the opening. In Figure 4, the laboratory setup is shown.



Figure 4. Reinforced concrete beam laboratory setup.

III. DISCUSSION AND EXAMINATION OF THE RESULTS

In the issue of usability of reinforced concrete structures, cracking and displacement are among the most critical parameters. Creating a crack and opening it in the reinforced concrete member will allow the penetration of moisture and destructive ions and will lead to the corrosion of the rebars. Apart from the problem of rebar corrosion, the existence of cracks or their creation, especially in reinforced concrete beams and slabs, greatly affects the safety and mental peace of users from the appearance point of view. This issue is so important that some researchers have evaluated the effect of cracking on rebar corrosion as less necessary in terms of psychological issues compared to its appearance.

Figure 5 shows the cracking pattern, and Figure 6 shows the load-displacement diagram for the laboratory samples.

The first sample that was tested was the C100 laboratory sample. For this purpose, the laboratory sample was placed under the jack, and loading started. Before the load of 50 kN, the load-displacement graph was linear, and no cracking was observed. At a load of 50 kN, the first hairline cracks were observed in the tensile part of the section and the middle of the beam opening. After that, with increasing loading, the graph became non-linear and oblique shear cracks were observed. Finally, at a load of 130 kilonewtons, after observing the cracks in the compressive part of the cross-section, and they became stronger in other terms, the diagram reached its maximum.

After that, the C75P25 laboratory sample was tested. In this sample, the first hairline cracks were observed at a load of 40 kN. After that, oblique cracks started to grow, and the load-displacement diagram entered the nonlinear stage. At the load of 80 kN and 110 kN, they started to grow and spread obliquely in the right support and the left support, respectively. At the final load of 136 kilonewtons, cracks were observed in the compressive part of the section, and other cracks became deeper and wider. In this sample, the largest crack was observed in the lower 75% of the beam section.

In the C50P50 laboratory sample, hairline cracks first occurred in the tensile part and the middle of the opening at a load of 45 kN. Then, these cracks grew and spread towards the supports. Finally, at the final load of 135 kilonewtons, cracks were observed in the compressive part of the section, and at this moment, the cracks became deeper. As seen in Figure 5, most of the cracks in this sample are vertical and occur in the middle of the opening. Also, in this sample, most of the cracks occurred in the lower 50%.

In the C25P75 laboratory sample, vertical and hairline cracks were first observed in the tensile part of the cross-section at a load of 40 kN. At the load of 60 kN, where the load-displacement diagram was almost nonlinear, almost oblique cracks were observed. At the load of 90 kilonewtons, cracks were observed on the sides of the right and left supports. Finally, at a load of 130 kilonewtons, when deep cracks were observed in the tensile and compressive parts of the section, the load-displacement diagram reached its maximum point.

In the P100 laboratory sample, the first hairline crack occurred at the load of 35 kN, and hairline cracks appeared in the bending opening of the beam, after which the load-displacement diagram entered the nonlinear stage. After that, the shear-bending cracks started to grow and expand towards the right and left supports. In such a way that at the load of 70 and 80 kilonewtons, cracks occurred near the supports. Finally, at a load of 130 kilonewtons, oblique cracks were observed in the compressive part of the beam section.

In the P75C25 laboratory sample, with increasing load, the amount of displacement in the middle of the beam span increased linearly until a vertical bending crack was observed at a load of 40 kN. After that, inclined cracks were observed at the load of 50, and the load-displacement diagram entered the nonlinear phase. As the load increased, the inclined cracks towards the supports started to grow and spread. Finally, at the final load of 142 kilonewtons, cracks were observed in the compression part of the section.

In the P50C50 laboratory sample, the first hairline crack was observed at a load of 50 kN, then oblique cracks were observed at a load of 60 kN, and the load-displacement diagram entered the nonlinear phase. After the load reached 80 kN, oblique cracks were observed in the compressive part of the section. As the loading increased, the cracks grew and spread until deep cracks were finally observed in the compressive area at a load of 130 kN. In this laboratory sample, most of the cracks were observed in the middle of the beam opening.

In the P25C75 laboratory sample, vertical cracks were first observed in the middle of the beam. At the load of 40 kN, the load-displacement diagram entered the nonlinear region, and at the load of 70 kN, oblique cracks were observed around the support on the lower part of the beam, and after that, the cracks grew and spread. At the load of 100 and 110 kN, oblique cracks were observed near the support, and finally, at the load of 135 kN, deep cracks were formed, and the load-displacement diagram reached its maximum.



Figure 5. Cracking pattern of reinforced concrete beam laboratory samples.

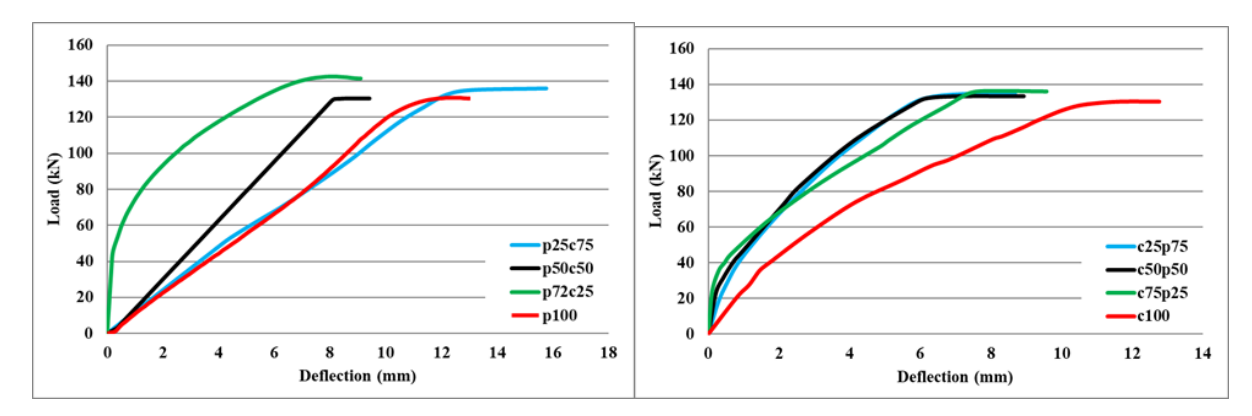


Figure 6. Load-displacement diagram of reinforced concrete beam laboratory samples.

As shown in Figure 5, the use of Hybrid Self-Compacting Pozzo-Lime concrete in the tension part of the beam section or the compression part will not affect the formation, growth, and expansion of cracks because the cracking pattern in the laboratory samples is almost the same. In other words, in these samples, the crack first formed in the tensile part and the middle of the opening of the laboratory samples, and then it spread towards the supports as the load increased.

According to Figure 5, in all the laboratory samples, the cracks in the middle of the opening are vertical, and the cracks around the support and under the load application points were oblique, which shows that the force transmission mechanism and the formation of threads Compressive and tensile in laboratory samples are almost the same.

Based on Figure 6, the values of final strength, hardness, ductility and depreciated energy of the laboratory samples have been obtained and are shown in Table 4.

As shown in Table 4, the lowest cracking load is related to the P100 laboratory sample, and its value is 35 kN. The highest cracking load is related to C100 and P50C50 samples, which is 50 kN.

Table 4.	Values of	of load an	d displacement	at vield	and ultimate i	noint.
I abic 4.	v arues c	oi ioau ai	u uisbiacemem	at viciu	anu unimaic i	וווטט

Specimens	Yield Point			Ultimate Point				
	F _Y (Kn)	Ratio of	D_{Y}	Ratio of	F _u (Kn)	Ratio of	D_u	Ratio of
		F_Y / F_{YReff}	(mm)	D_Y/D_{YReff}		F_U/F_{UReff}	(mm)	D_U / D_{UReff}
C100(Reff)	50	1	2.41	1	130.50	1	12.78	1
C75P25	40	0.8	0.46	0.19	136.24	1.04	8.14	0.64
C50P50	45	0.9	0.91	0.38	133.38	1.02	8.94	0.7
C25P75	40	0.8	0.75	0.31	134.76	1.03	8.69	0.68
P100	35	0.7	3.15	1.31	130.67	1.001	12.69	0.99
P75C25	40	0.8	0.17	0.07	142.43	1.09	8.05	0.63
P50C50	50	1	3.21	1.33	130.65	1.001	8.48	0.66
P25C75	40	0.8	3.50	1.45	135.95	1.04	15.78	1.23

Table 5. Values of Stiffness, ductility and energy dissipated.

Specimens	Stiffness (F _{cr} /D _{cr})	Ductility (D _u /D _{cr})	Energy Dissipated (Kn.mm)
C100	20.75	5.30	1121.62
C75P25	86.96	17.69	950.98
C50P50	49.45	9.82	897.40
C25P75	53.33	11.59	854.11
P100	11.11	4.03	955.99
P75C25	235.29	47.33	1039.25
P50C50	15.58	2.64	687.35
P25C75	11.43	4.51	1321.23

Ultimate strength is one of the important parameters for designing reinforced concrete structures. For this reason, its value is obtained based on the load-displacement diagram. The ultimate resistance in this research is equal to the maximum point in the load-displacement diagram. The final strength values of the laboratory samples of reinforced concrete beams are shown in Table 4.

According to Figure 7, the highest final strength corresponds to the P75C25 laboratory sample, and its value is 142.43 kN. Also, the lowest value of the last resistance is related to the laboratory samples C100, P100, and P50C50, which is about 130 kilonewtons.

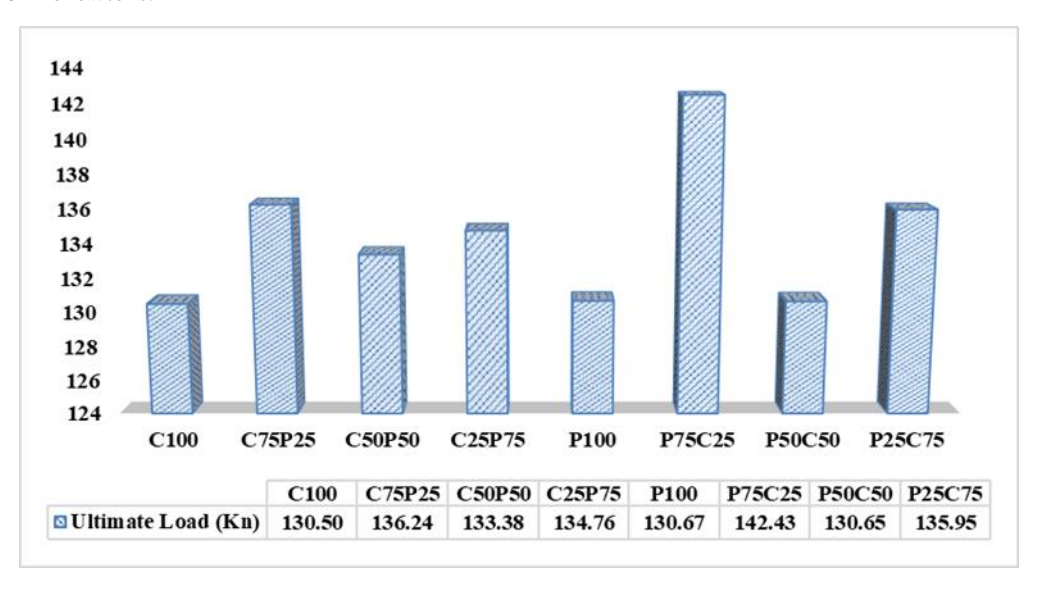


Figure 7. Ultimate load values for laboratory samples.

The hardness of the reinforced concrete beam is its resistance to deformation. The use of special concretes, such as self-compacting concrete, is one of the ways to increase the hardness of the structure against lateral forces and prevent damage to it. In this research, in order to check the initial hardness of the laboratory samples and compare the hardness of each sample with other samples, the initial slope of the force-displacement curve has been used as a criterion for evaluation between the samples. The bar graph of the hardness of the laboratory samples is shown in Figure 8.

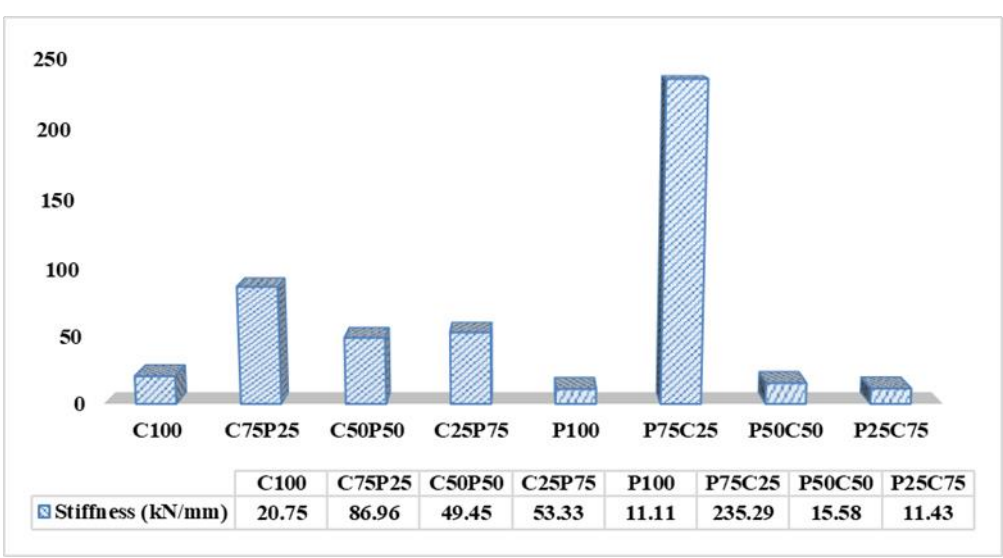


Figure 8. Hardness values for laboratory samples.

According to Figure 8, the hardness of the P75C25 laboratory sample is 235.29 kN/mm. Also, the lowest hardness is related to the P100 laboratory sample.

Deformation capacity is an important index in the seismic behaviour of reinforced concrete beams, which is defined by the displacement ductility factor and as the ratio of ultimate limit displacement to yield limit displacement. To the extent that the ductility is high, the structure can withstand large deformations before breaking. In Figure 9, the amount of

plasticity of laboratory samples is shown. As can be seen, the P75C25 laboratory sample has the highest ductility value, which is around 47.33. According to the recommendations of international regulations, the minimum ductility value of reinforced concrete beam should be around 8, which, in this research, the minimum ductility of samples P50C50, P100, P25C75, and C100 is not acceptable.

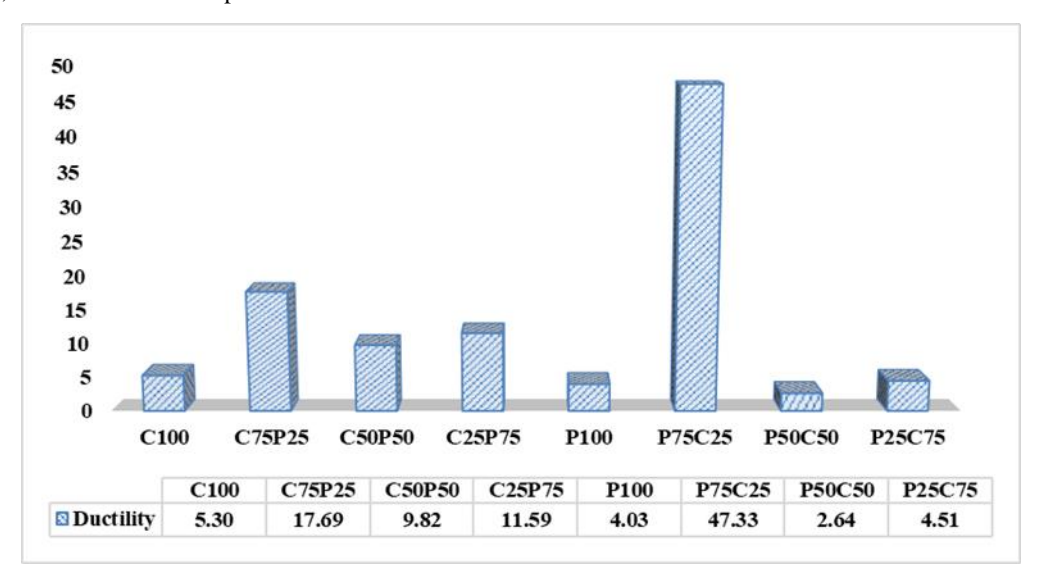


Figure 9. Ductility values for laboratory samples.

The wasted energy is the area under the load-displacement diagram. To the extent that the depreciated energy of the structure is high, it is less damaged during an earthquake. In Figure 10, the amount of wasted energy of the laboratory samples is shown.

According to Figure 10, the highest amount of dissipated energy corresponds to the P25C75 laboratory sample. Its value is 1321.23 kN/m, and the lowest amount of dissipated energy equals 681.35, which corresponds to the P50C50 laboratory sample.

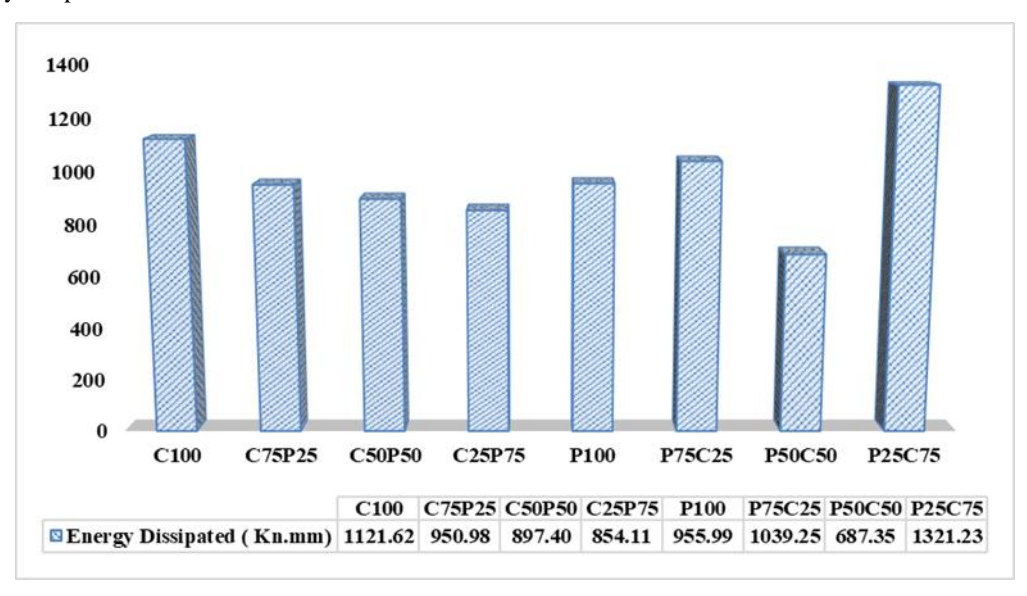


Figure 10. Dissipated energy values for laboratory samples.

IV. CONCLUSIONS

Understanding and knowing the bending behaviour of reinforced concrete beams is very complex and vital, and this importance will increase if Hybrid Self-Compacting Pozzo-Lime reinforced concrete is used. Many studies and experiments have been conducted in the field of examining reinforced concrete beams under bending, but in the field of studying the bending behaviour of hybrid self-compacting Pozzo-Lime reinforced concrete beams, the experiments are much less and more limited. The main purpose of this thesis is to investigate the behaviour of reinforced concrete beams with Hybrid Self-Compacting Pozzo-Lime reinforced concrete under-bending effect. In this regard, the first eight beams with a length of 1400 mm were made. After testing these samples, a load-displacement diagram was obtained for them,

based on which the final strength, hardness, ductility and depreciated energy were discussed and investigated. Also, the cracking patterns in the laboratory samples of reinforced concrete beams were compared with the laboratory results. The results of this research are summarised as follows.

- 1- The use of Hybrid Self-Compacting Pozzo-Lime concrete in the tension part of the beam section or the compression part will not affect the formation, growth, and expansion of cracks.
- 2- The highest final strength corresponds to the P75C25 laboratory sample, and its value is 142.43 kN. Also, the lowest value of the final resistance is related to the laboratory samples C100, P100, and P50C50, which is about 130 kilonewtons.
- 3- The highest hardness corresponds to the laboratory sample P75C25, whose value is 235.29 kN/mm. Also, the lowest hardness is related to the P100 laboratory sample.
- 4- The laboratory sample P75C25 has the highest plasticity value; its amount is about 47.33. According to the recommendations of international regulations, the minimum ductility value of reinforced concrete beam should be around 8, which, in this research, the minimum ductility of samples P50C50, P100, P25C75, and C100 is not acceptable.
- 5- The highest amount of consumed energy corresponds to the P25C75 laboratory sample, and its value is 1321.23 kN/m, and the lowest amount of consumed energy equals 681.35, which corresponds to the P50C50 laboratory sample.
- 6- Considering that the lowest final strength corresponds to the laboratory samples C100, P100, and P50C50 and the lowest plasticity value corresponds to the samples P100, P25C75, and C100, it is recommended to use beams with such details in the design of structures avoided.
- 7- Considering that the highest final strength, the highest hardness and the highest ductility are related to the laboratory sample of the P75C25 beam, it can be said that the best way to use Hybrid Self-Compacting Pozzo-Lime reinforced concrete in the reinforced concrete beam is when This type of concrete should be used for 75% of the beam section from the bottom.

REFERENCES

- [1] Zhang, Z., Xiao, J., Zhang, Q., Han, K., Wang, J., Hu, X., A state-of-the-art review on the stability of self-consolidating concrete. Construction and Building Materials, 268, 121099, 2021.
- [2] Liu, Y.-X., Ling, T.-C., Mo, K.-H., Progress in developing self-consolidating concrete (SCC) constituting recycled concrete aggregates: A review. International Journal of Minerals, Metallurgy and Materials, 28, 522-537, 2021.
- [3] Meko, B., Ighalo, J. O., Ofuyatan, O. M., Enhancement of self-compactability of fresh self-compacting concrete: A review. Cleaner Materials, 1, 100019, 2021.
- [4] Pang, L., Liu, Z., Wang, D., An, M., Review on the application of supplementary cementitious materials in self-compacting concrete. Crystals, 12(2), 180, 2022.
- [5] Faraj, R. H., Ali, H. F. H., Sherwani, A. F. H., Hassan, B. R., Karim, H., Use of recycled plastic in self-compacting concrete: A comprehensive review on fresh and mechanical properties. Journal of Building Engineering, 30, 101283, 2020.
- [6] Dey, S., Kumar, V. P., Goud, K., Basha, S., State of art review on self compacting concrete using mineral admixtures. Journal of Building Pathology and Rehabilitation, 6(1), 18, 2021.
- [7] Ramkumar, K., Rajkumar, P. K., Ahmmad, S. N., Jegan, M., A review on performance of self-compacting concrete—use of mineral admixtures and steel fibres with artificial neural network application. Construction and Building Materials, 261, 120215, 2020.
- [8] Revilla-Cuesta, V., Skaf, M., Faleschini, F., Manso, J. M., Ortega-López, V., Self-compacting concrete manufactured with recycled concrete aggregate: An overview. Journal of Cleaner Production, 262, 121362, 2020.
- [9] Shokravi, H., Mohammadyan-Yasouj, S. E., Koloor, S. S. R., Petrů, M., Heidarrezaei, M., Effect of alumina additives on mechanical and fresh properties of self-compacting concrete: A review. Processes, 9(3), 554, 2021.
- [10] Singh, A., Duan, Z., Xiao, J., Liu, Q., Incorporating recycled aggregates in self-compacting concrete: a review. Journal of Sustainable Cement-Based Materials, 9(3), 165-189, 2020.
- [11] Singh, N., Kumar, P., Goyal, P., Reviewing the behaviour of high volume fly ash based self compacting concrete. Journal of Building Engineering, 26, 100882, 2019.
- [12] Vahidi, E.K., Moradi, R., Numerical study of the force transfer mechanism and seismic behavior of masonry infilled RC frames with windows opening. Civil Engineering Journal, 5(1), 61-73, 2019.

- [13] Moradi, R., Khalilzadeh Vahidi, E., Comparison of Numerical Techniques of Masonry Infilled RC Frames for Lateral Loads. Journal of Concrete Structures and Materials, 3(2), 102-118, 2018.
- [14] Moradi, R., Khalilzadeh Vahidi, E., General Study of New Ideas and Practical of Friction Dampers for Passive Vibration Control of Structures. Karafan Quarterly Scientific Journal, 17(4), 239-257, 2021.
- [15] Moradi, R., Khalilzadeh Vahidi, E., Experimental Study of Rotational-Friction Damper with Two Slip Load and Evaluation of its Performance in RC Frame under Cyclic Loading. Journal of Concrete Structures and Materials, 6(1), 121-137, 2021.
- [16] Ashish, D. K., Verma, S. K. An overview on mixture design of self-compacting concrete. Structural Concrete, 20(1), 371-395, 2019.
- [17] Santos, S., Da Silva, P., De Brito, J., Self-compacting concrete with recycled aggregates—a literature review. Journal of Building Engineering, 22, 349-371, 2019.
- [18] Mujedu, K. A., Ab-Kadir, M. A., Ismail, M., A review on self-compacting concrete incorporating palm oil fuel ash as a cement replacement. Construction and Building Materials, 258, 119541, 2020.
- [19] Nakagawa N, Yamashita T. Comparative study of traditional face-to-face teaching, audience response system, and a flipped classroom plus audience response. Journal of Advanced Pharmacy Education and Research. 2022;12(1-2022):9-16.
- [20] Rohmani S, Desi BA, Wardhani WD. Potassium-Azeloyl-Diglycinate BB-Cream formulation with Triethanolamine variation, and its effects on In-Vitro SPF stability and values. Journal of Advanced Pharmacy Education and Research. 2022;12(1-2022):1-8.
- [21] Singh GP, Attavar SH, Kavuri S. Application of Cone-Beam Computed Tomography in Diagnosis and Treatment of Multiple Canals—A Case Report. Annals of Dental Specialty. 2022;10(2-2022):15-8.
- [22] Nguyen DT, Hoang TH. Impact of capabilities on operational performance: The case of vietnamese enterprises. Journal of Organizational Behavior Research. 2022;7(2):73-81.
- [23] Albiajawi, M. I., Embong, R., Muthusamy, K., Influence of Mineral Admixtures on the Properties of Self-Compacting Concrete: An Overview. Construction, 1(2), 62-75, 2021.
- [24] Adesina, A., Performance and sustainability overview of alkali-activated self-compacting concrete. Waste Disposal & Sustainable Energy, 2(3), 165-175, 2020.
- [25] Nawaz, W., Elchalakani, M., Yehia, S., Xie, T., Liu, H., Yang, B., et al., Shear strengthening performance of GFRP reinforced lightweight SCC beams: Experimental and analytical study. Engineering Structures, 278, 115545, 2023.
- [26] Mansi, A., Sor NH, Hilal, N., Qaidi, S. M., editors., The impact of nano clay on normal and high-performance concrete characteristics: a review, IOP Conference Series: Earth and Environmental Science, IOP Publishing, 2022
- [27] Saha, P., Meesaraganda, L. V., Experimental investigation of reinforced SCC beam-column joint with rectangular spiral reinforcement under cyclic loading. Construction and Building Materials, 201, 171-185, 2019.
- [28] Afshoon, I., Miri, M., Mousavi, S. R., Evaluating the flexural behavior of green copper slag-contained steel fiber reinforced SCC beams with/without initial notches. Construction and Building Materials, 395, 132316, 2023.
- [29] Kassimi, F., El-Sayed, A. K., Khayat, K. H., Flexural behavior of fiber-reinforced SCC for monolithic and composite beams. Journal of Advanced Concrete Technology, 19(8), 937-949, 2021.
- [30] Ashteyat, A. M., Haddad, R., Obaidat, Y. T., editors, Repair of heat-damaged SCC cantilever beams using SNSM CFRP strips. Structures, 24, 151-162, 2020.